Runx1-mediated hematopoietic stem-cell emergence is controlled by a Gata/Ets/SCL-regulated enhancer

Wade T. Nottingham,[1] Andrew Jarratt,[1] Matthew Burgess,[1] Caroline L. Speck,[1] Jan-Fang Cheng,[2,3] Shyam Prabhakar,[2,3] Eddy M. Rubin,[2,3] Pik-Shan Li,[1] Jackie Sloane-Stanley,[1] John Kong-a-San,[4] and Marella F. T. R. de Bruijn[1]

[1]Medical Research Council (MRC) Molecular Haematology Unit, Weatherall Institute of Molecular Medicine, John Radcliffe Hospital, Oxford, United Kingdom; [2]Genomics Division, Lawrence Berkeley National Laboratory, Berkeley, CA; [3]United States Department of Energy Joint Genome Institute, Walnut Creek, CA; and [4]Department of Cell Biology, Erasmus Medical Center, Rotterdam, The Netherlands

The transcription factor *Runx1/AML1* is an important regulator of hematopoiesis and is critically required for the generation of the first definitive hematopoietic stem cells (HSCs) in the major vasculature of the mouse embryo. As a pivotal factor in HSC ontogeny, its transcriptional regulation is of high interest but is largely undefined. In this study, we used a combination of comparative genomics and chromatin analysis to identify a highly conserved 531-bp enhancer located at position + 23.5 in the first intron of the 224-kb mouse *Runx1* gene. We show that this enhancer contributes to the early hematopoietic expression of *Runx1*. Transcription factor binding in vivo and analysis of the mutated enhancer in transient transgenic mouse embryos implicate Gata2 and Ets proteins as critical factors for its function. We also show that the SCL/Lmo2/Ldb-1 complex is recruited to the enhancer in vivo. Importantly, transplantation experiments demonstrate that the intronic *Runx1* enhancer targets all definitive HSCs in the mouse embryo, suggesting that it functions as a crucial *cis*-regulatory element that integrates the Gata, Ets, and SCL transcriptional networks to initiate HSC generation. (Blood. 2007;110:4188-4197)

Introduction

The interest in stem cell–based therapies has emphasized the importance of understanding the molecular mechanisms by which cells choose their fate and mature along a particular lineage. The hematopoietic system has been particularly amenable for these type of studies, and preliminary gene regulatory networks have been generated to summarize and model the data obtained from a variety of in vitro and in vivo studies.[1,2] However, few studies have directly addressed the transcriptional regulation of critical hematopoietic regulators at the stages at which they are active (ie, during hematopoietic stem cell [HSC] formation in embryonic development). The transcription factor (TF) Runx1 (also known as AML1, Cbfa2, or Pebp2α) is arguably the most critical regulator of definitive HSC formation and is a frequent target of chromosomal translocations in leukemia (reviewed in de Bruijn and Speck[3]; Jaffredo et al[4]; and Speck and Gilliland[5]). To advance our understanding of the molecular mechanisms involved in the process of HSC specification, it is thus of great interest to determine how *Runx1* expression is regulated, particularly in HSC fated precursor cells. Very little is known concerning the transcriptional regulation of *Runx1*. Although several signaling pathways and TFs have been reported to act upstream of *Runx1* in the development of the hematopoietic system (reviewed in Levanon and Groner[6]),[7-15] no *cis*-regulatory elements have been identified. In the present study, we set out to identify and functionally characterize *Runx1 cis*-elements that are sufficient to drive reporter gene expression specifically to the sites of HSC emergence in a *Runx1*-specific pattern. Identification of such element(s) is a prerequisite to place the master regulator Runx1 firmly in the transcriptional network governing HSC emergence.

Materials and methods

Identification of conserved noncoding elements (CNEs)

Genomic sequences spanning the *Runx1* locus were obtained from the NCBI (mouse build 36; human build 36)[16] and Ensembl (*Xenopus tropicalis* JGI 4.1; CanFam1.0)[17] databases, and by the sequencing and assembly of BACs containing opossum and chicken *Runx1* following standard procedures (clones LBNL3_236F8, LBNL3_175O22, LBNL3_86F2, and CHORI-261_61E4). Opossum and chicken sequences are available through accession numbers AC146773, AC148232, AC151874, and AC146486. The mouse genomic sequence served as the base for sequence alignments using M-LAGAN (http://genome.lbl.gov/vista/index.shtml[18,19]) and MultiPipmaker (http://pipmaker.bx.psu.edu/pipmaker/[20]). The Gumby algorithm was used to identify CNEs with high likelihood of *cis*-regulatory function (available through the Vista website).[21] Putative TF-binding sites were identified using JASPAR matrices.[22] Alignments of individual CNEs were generated using ClustalX (MacVector; Accelrys, Cary, NC).

Timed matings and embryo collection

For timed pregnancies, female (129S1 × C57BL/6)F1 mice were mated overnight (O/N) with (129S1 × C57BL/6)F1, + *23-line1* Tg, or *Runx1-LacZ* KI males and checked for vaginal plugs the next morning (E0) ($Runx1^{lz/+}$ mice kind gift of N. Speck, Dartmouth Medical School, Hanover, NH[23]). $Runx1^{lz/+}$ and + *23-Line1* Tg mice were maintained on a mixed background (129S1 × C57BL/6 and CBA × C57BL/6, respectively). Mice were housed with free access to food and water. All procedures were in

Submitted July 11, 2007; accepted September 3, 2007. Prepublished online as *Blood* First Edition paper, September 6, 2007; DOI 10.1182/blood-2007-07-100883.

The online version of this article contains a data supplement.

The publication costs of this article were defrayed in part by page charge payment. Therefore, and solely to indicate this fact, this article is hereby marked "advertisement" in accordance with 18 USC section 1734.

compliance with Home Office regulations. Embryos were collected in phosphate-buffered saline (PBS; Gibco, Paisley, United Kingdom) supplemented with 10% fetal calf serum (Biosera, East Sussex, United Kingdom), 50 U/mL penicillin, and 50 μg/mL streptomycin (Gibco) (PBS-FSC).

Cell culture

The mouse 416B myeloid progenitor cell line (kind gift of T. Enver, MRC Molecular Hematology Unit, Oxford, United Kingdom) was grown in Fischer medium (Gibco) supplemented with 20% horse serum (Gibco), 2 mM L-glutamine (Gibco), 50 U/mL penicillin, and 50 μg/mL streptomycin (Cambrex Bioscience, Cambridge, United Kingdom), at 37°C, 5% CO_2. Cells were maintained at a density of 2 to 8 × 10^5 cells/mL.

DHS analysis

DNAseI hypersensitive site (DHS) analysis was carried out as described.[24] Briefly, isolated nuclei of (129S1 × C57BL/6)F2 E12 fetal liver (FL) and 416B cells were treated with increasing amounts of DNaseI (Roche, Burgess Hill, United Kingdom; 5 to 160 U and 0.5 to 16 U/sample, respectively). DNA was isolated and digested with appropriate restriction enzymes, and 5- to 15-kb restriction fragments were analyzed by Southern blot using single-copy probes located at the 5′ or 3′ end of the restriction fragments. Positions of restriction fragments, probes, and corresponding primer sequences are available upon request. All primers were designed using Primer3 (http://primer3.sourceforge.net/, Whitehead Institute for Biomedical Research, Cambridge, MA).

Luciferase and LacZ enhancer-reporter constructs

Genomic fragments spanning (parts of) the + 23 CNE were generated by polymerase chain reaction (PCR) (Table S2, available on the *Blood* website; see the Supplemental Materials link at the top of the online article). Fragments were cloned downstream of the *Luciferase* gene in the pGL3-Promoter vector (Promega, Southampton, United Kingdom) or downstream of the *LacZ* gene in an *hsp68LacZ* reporter vector (kind gift of D. Meijer, Erasmus Medical Center, Rotterdam, The Netherlands; maps available on request). Mutagenesis of putative TF-binding sites in the *pGL3P + 23* and the *hsp68LacZ + 23* constructs was carried out using the QuickChange Site Directed Mutagenesis Kit (Stratagene Europe, Amsterdam, The Netherlands; Table S3). Mutations were confirmed by sequencing.

Analysis of enhancer activity in F0 transgenic mouse embryos

Mouse F0 transgenic embryos carrying *LacZ* enhancer-reporter constructs were generated by pronuclear injection of (C57BL/6 × CBA)F2 zygotes following standard procedures. Transgenic embryos were identified by *LacZ*-specific PCR on genomic DNA isolated from YS/ectoplacental cone (5′-GCAGATGCACGGTTACGATG-3′; 5′-GTGGCAACATG-GAAATCGCTG-3′). Embryos were fixed for 30 minutes to 1 hour at 4°C in 1% formaldehyde (VWR International, Lutterworth, United Kingdom), 0.2% glutaraldehyde (Sigma, Poole, United Kingdom), 2 mM $MgCl_2$, 5 mM EGTA (pH 8.0), and 0.02% NP-40 in PBS; washed in 0.02% NP-40 in PBS; and stained O/N at room temperature (RT) in the dark in Xgal staining solution (5 mM $K_3Fe(CN)_6$, 5 mM $K_4Fe(CN)_6$·3 H_2O, 2 mM $MgCl_2$, 0.01% sodium deoxycholate, 0.02% nonidet P-40 [NP-40], and 1 mg/mL Xgal [5-Bromo-4-chloro-3-indolyl-D-galactopyranoside; Sigma] in PBS). Embryos were washed in PBS, postfixed O/N at 4°C, photographed using a Leica MZFLIII microscope, Leica DFC 300F digital camera (Leica Microsystems, Milton Keynes, United Kingdom) and Openlab software (Improvision, Coventry, United Kingdom), incubated O/N at 4°C in 15% sucrose in PBS, and embedded in Tissue-Tek OCT compound (Sakura, Siemens Medical Solutions Diagnostics, Newbury, United Kingdom). Transverse sections (8-10 μm) were cut on a Leica CM3050S Cryostat (Leica Microsystems), coverslipped using Kaiser glycerol gelatin (VWR International), and examined using a Nikon Eclipse E600 microscope (Nikon, Tokyo, Japan). Pictures were made with an Olympus Camedia C-3030 Zoom digital camera (Olympus, Melville, NY) and Adobe Photoshop (Adobe Systems Europe, Uxbridge, United Kingdom).

Luciferase assays

Luciferase assays were performed as described[25] with minor modifications. Briefly, 10^7 416B cells were electroporated with 10 μg test plasmid and 1 μg pRL-TK control plasmid (Promega) at 220 V and 960 μFD. Relative luciferase activity was determined after 24 hours using the Dual Luciferase Reporter Kit (Promega). Luciferase activity was measured on a FLUOstar Optima luminometer (BMG Labtech, Aylesbury, United Kingdom). The ratio of firefly over renilla luciferase activity was used to correct for transfection efficiency.

ChIP and real-time PCR

For chromatin immunoprecipitation (ChIP) assays, 10^7 416B cells were incubated in 0.5% formaldehyde in media for 10 minutes at RT to cross-link DNA and protein and processed as described.[24] Chromatin was sonicated to produce fragments of 300 to 500 bp. ChIP was performed using the ChIP Assay Kit (Upstate Biotechnology, Millipore, Amsterdam, The Netherlands). Antibodies used in ChIP were Elf-1 (sc-631X; Santa Cruz, Santa Cruz, CA), Fli-1 (sc-356X; Santa Cruz), Gata2 (sc-9008; Santa Cruz), Ldb1, Lmo2, SCL (kind gifts of C. Porcher, MRC Molecular Hematology Unit, Oxford), Pu.1 (sc-352; Santa Cruz), and Runx1 (N-terminus, PC284L; Calbiochem, San Diego, CA). Relative enrichment of target sequences was measured by real-time PCR as described,[24] using primers and 5′FAM-3′TAMRA–labeled probes selected from unique sequences within the *Runx1* locus (Table S4, available on the *Blood* website, see the Supplemental Materials link at the top of the online article).

Flow cytometry

E11 aorta-gonad-mesonephros (AGM) region, vitelline and umbilical arteries (VUs), and FL were dissected in PBS-FSC. The dorsal aorta with its surrounding mesenchyme was subdissected free from the urogenital ridges and combined with VU (AVU). At the time of dissection, + *23-Line1* Tg embryos were discriminated from wild-type littermates by incubating severed heads in Xgal staining solution (see "Analysis of enhancer activity in FD transgenic embryos") for 2 hours at 37°C. Tissues were pooled according to genotype and cell suspensions made as described.[26,27] Viable cells were counted using Trypan Blue (Sigma) and a Neubauer hemocytometer (VWR International). On average, 37.6 (± 9.6) × 10^4 (mean ± SD; n = 14) and 42.3 (± 8.9) × 10^4 (n = 10) cells were obtained from E11 AVU and FL, respectively.

Cell suspensions of E11 AVU and FL were loaded with fluorescein di-β-D-galactopyranoside (FDG; Molecular Probes, Leiden, the Netherlands) as described.[28] FDG was detected in the FL1 channel of a MoFlo flow cytometer (Dako, Ely, United Kingdom). Dead cells and debris were excluded from the analyses and sorts on the basis of Hoechst 33258 uptake and forward scatter characteristics. FDG^- and FDG^+ sorted cells from + *23-Line1* Tg tissues were collected in 100% 0.45-μm filtered FCS and washed in PBS, and viable cells were counted using a Neubauer hemocytometer.

Analysis of hematopoietic activity

Clonogenic progenitor cells within the sorted FL and AVU cell populations were assayed in the colony-forming unit–culture (CFU-C) assay. Cells were plated in duplicate in 35-mm culture dishes in MethoCult M3434 (StemCell Technologies, London, United Kingdom) according to the manufacturer's instructions. Cultures were grown at 37°C, 5% CO_2 and colonies counted after 7 days.

FDG^- and FDG^+ FL and AVU cell populations were assayed for the presence of definitive HSCs as described.[26] Briefly, adult male (C57BL/6 × CBA)F1 mice were conditioned with a split dose of 9 Gy from a ^{137}Cs source. Embryonic cells were coinjected with 2 × 10^5 (C57BL/6 × CBA)F1 spleen cells (to promote survival). Recipients were analyzed for donor-derived hematopoietic reconstitution at 1 to 2 and more than 4 months after transfer by *LacZ*-specific semiquantitative PCR on peripheral blood DNA. Multilineage hematopoietic reconstitution was assessed as described.[27]

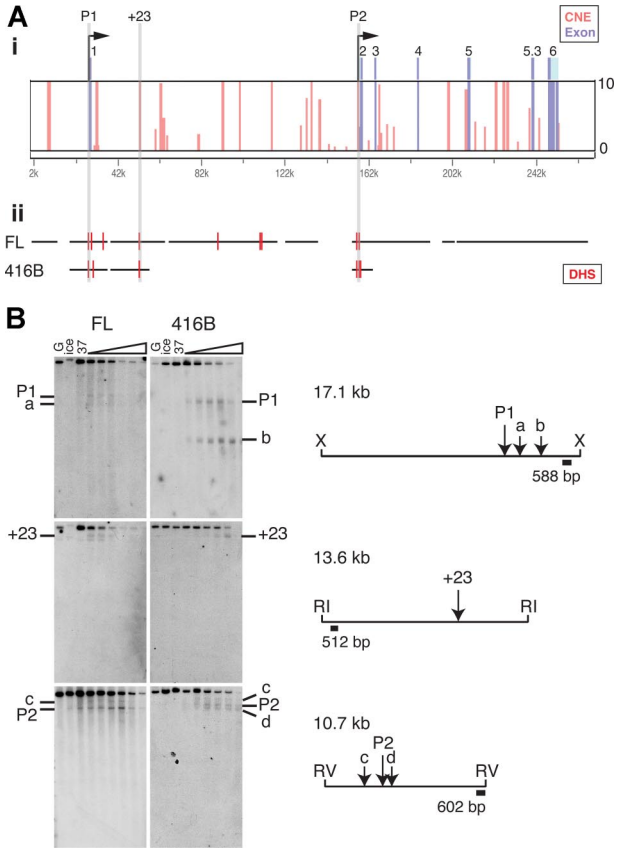

Figure 1. Identification of candidate *cis*-elements in the mouse *Runx1* locus. (A) Gumby output and DHS (Chr 16: 92473100–92743100 spanning *Runx1* plus 30 kb upstream and 15 kb downstream; NCBIM build 36). (i, top) Position of *Runx1* exons (numbered according to Levanon and Groner[6]; coding sequence [dark blue], UTRs [light blue]). Gumby-identified CNEs (pink) and exons (blue) are shown as colored bars. Height of bars shows $-\log_{10}(P \text{ value})$ (cutoff at 10). (ii) Hematopoietic DHS detected along the mouse *Runx1* locus (vertical red bars) in the area analyzed (horizontal black lines). Only 3 CNEs with a $-\log_{10}(P \text{ value})$ more than 10 corresponded to a DHS (light gray shading; P1 CNE not visible on this scale, Table S1). (B) Southern blots for P1, + 23, and P2 DHSs in E12 FL and 416B (nuclei treated with increasing concentrations of DNAseI [triangles]). G indicates genomic control; 0^{ice}, DNaseI free ice; and 0^{37}, DNAse I free 37°C controls. Restriction maps (to scale) with positions and sizes of probes (▬) and DHSs (⇩) are shown next to each set of blots. DHS mapping to the P1, + 23, and P2 CNE are indicated. Additional DHSs (not discussed in this paper) are labeled a-d. X indicates *Xba*I; RI, *Eco*RI; and RV, *Eco*RV.

Results

Identification of candidate hematopoietic *Runx1 cis*-regulatory elements

To identify conserved noncoding elements (CNEs) with a high likelihood of *cis*-regulatory function in the *Runx1* locus, we performed Gumby analysis[21] of a 6-way Multi-LAGAN[18,19] alignment of 270 kb of mouse genomic sequence spanning *Runx1,* and corresponding genomic sequences of human *(Homo sapiens),* dog *(Canis familiaris),* opossum *(Monodelphis domestica),* chicken *(Gallus gallus),* and frog *(Xenopus tropicalis).* Gumby identified 42 CNEs in the *Runx1* locus, 13 of which had *P* values less than le–10 (ie, a high likelihood of *cis*-regulatory function[21]; Figure 1Ai). The *Runx1* P1 and P2 promoter regions were among these (Table S1), confirming that relevant *Runx1 cis*-elements can be found in this manner. We then performed DNAseI hypersensitive site (DHS) analysis on E12 mouse FL (harboring Runx1$^+$ hematopoietic cells[28]) to select those candidate *cis*-elements that are in an open chromatin configuration in hematopoietic progenitor cells. Approximately 85% of the 270 kb mouse *Runx1* locus was analyzed and 9 DHSs were identified, only 3 of which mapped precisely to Gumby CNEs with low *P* values, namely the *Runx1* P1 and P2 promoter regions and an intronic 194-bp mouse-frog conserved CNE located 23.5-kb downstream of the ATG in exon1 (named + 23) (Figure 1A,B; Table S1). All 3 DHSs were confirmed in 416B myeloid progenitor cells (*Runx1*-positive by RT-PCR, not shown; Figure 1A,B, Table S1). Since in vitro and preliminary in vivo analysis of P1 and P2 promoter fragments had indicated that the *Runx1* promoters lack clear tissue specificity (Ghozi et al[29]; D. Levanon and Y. Groner, Weizmann Institute of Science, oral communication; T. Bee and M.F.T.R.B., unpublished observations, 2006); we focused on the + 23 CNE as a candidate hematopoietic-specific *Runx1 cis*-element.

The + 23 CNE has hematopoietic *Runx1*-specific enhancer activity in the mouse embryo

To assess whether the + 23 CNE has enhancer activity at hematopoietic sites of the embryo in a pattern relevant to endogenous *Runx1,* a 531-bp mouse genomic fragment containing the + 23 CNE was cloned downstream of the *LacZ* gene in an *hsp68LacZ* reporter construct (the *hsp68* promoter alone did not drive reproducible hematopoietic *lacZ* expression [Figure S1]). F0 *hsp68LacZ + 23* transgenic embryos were generated and analyzed for *LacZ* expression at E8 and E10. At these time points, the + 23 CNE consistently showed enhancer activity at hematopoietic sites (Figure 2A). In 4 of 5 E8 embryos, the + 23 CNE targeted expression to cells in the yolk sac (YS) blood islands (BIs) and to the paired dorsal aortae in the para-aortic splanchnopleura (PAS; Figure 2Bi-iv). In addition, *LacZ* expression was seen in the anterior aortae (Figure 2Bi black arrowhead). Comparison with a *Runx1-LacZ* KI[23] mouse line showed that the pattern of enhancer activity in the E8 hematopoietic territories (ie, YS BIs and PAS) resembles the endogenous *Runx1* expression pattern (Figure 2Bv-viii). At E10, the + 23 enhancer was active in the AGM (PAS derivative) and the VU of 5 of 11 and 4 of 11 expressing embryos, respectively (Figure 2A). Here, + 23 particularly targeted the hematopoietic cell clusters attached to the walls of these arteries (arrowheads Figure 2Ci,ii and Figure S2A). These clusters are the sites where the first definitive HSCs of the embryo are found.[27,28] In addition, enhancer activity was observed in a small subset of endothelial cells (often underlying the clusters), and in some cells in the mesenchyme under the aorta (Figure 2Ci,ii arrows). This pattern of activity is consistent with endogenous *Runx1* expression in these arteries, although, remarkably, the + 23 enhancer did not recapitulate the wider endothelial and mesenchymal expression seen in the aorta of *Runx1-LacZ* KI embryos[23,28] (Figure 2Cv). In the YS, the + 23 enhancer targeted blood cells in the YS capillaries as seen in the *Runx1-LacZ* KI (compare Figure 2Ciii and Cvii), and in the developing FL some individual hematopoietic cells expressed *LacZ,* but no expression was seen in the liver capsule (compare Figure 2Civ and Cviii). Furthermore, *LacZ*$^+$ cells were found in the placenta (Figure S2B as described for the Runx1-lacZ KI[30,31]).

+ 23 enhancer activity in 416B cells is controlled by Runx, Gata, and Ets motifs

To characterize the regulatory modules that control the activity of the + 23 enhancer in hematopoiesis, we generated an enhancer deletion series in the enhancerless pGL3P vector (Figure 3A).

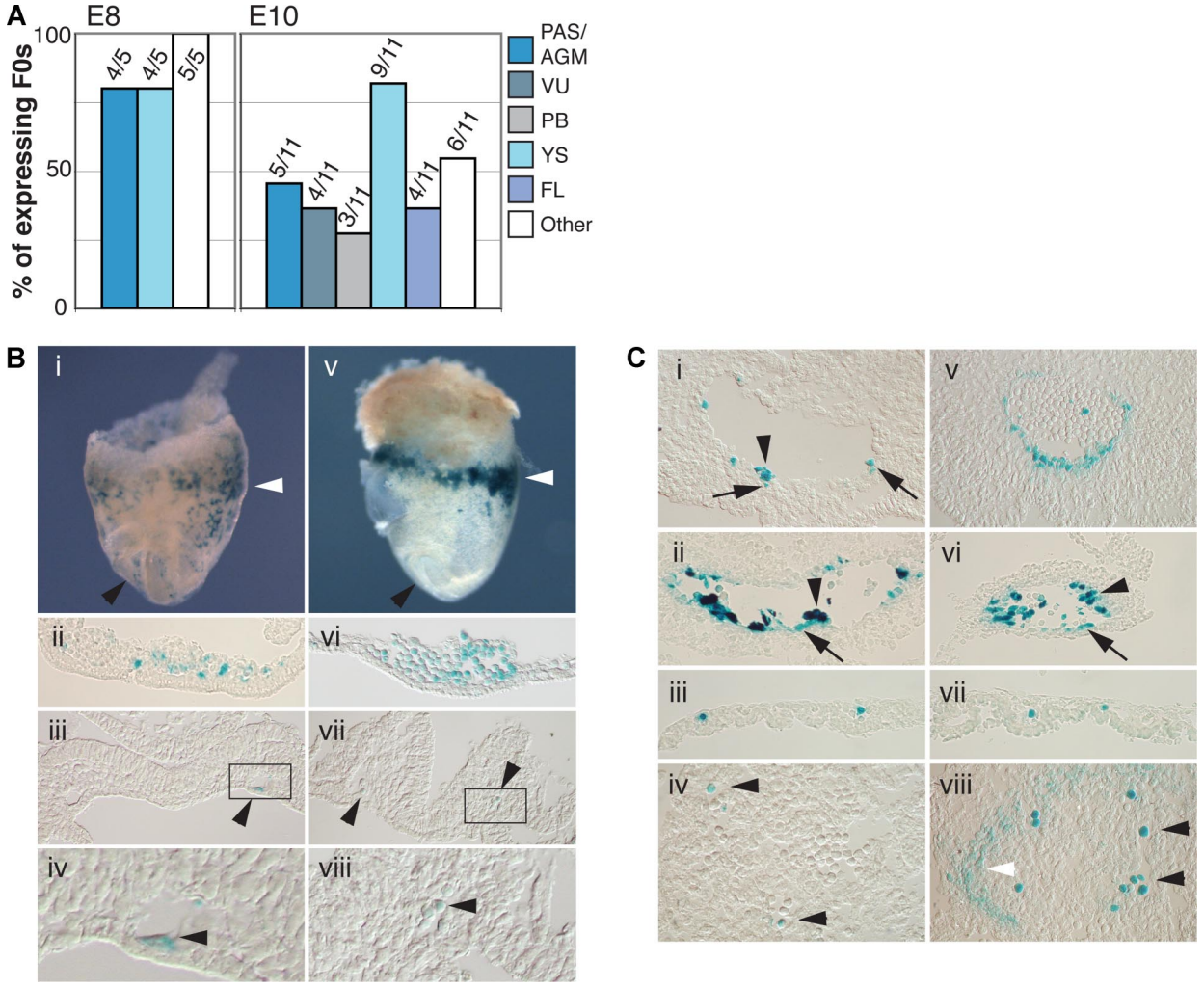

Figure 2. The + 23 CNE shows *Runx1*-related enhancer activity in hematopoietic tissues of the mouse embryo. (A) Summary of + 23 enhancer activity in *lacZ*-expressing F0 *hsp68LacZ* + *23* transgenic embryos. Data show the number and percentage of embryos in which *LacZ* expression was found in the indicated tissue. "Other" represents ectopic, nonreproducible expression outside the hematopoietic system, presumably resulting from random integration of the constructs at or near endogenous enhancers. (B) *LacZ* expression in early E8 (5-6 sp) *hsp68LacZ* + *23* F0 transgenic (i-iv) and *Runx1-lacZ* KI (v-viii) embryos. (i,v) *LacZ* expression in whole mounts. White arrowheads point at the area of the BI; black arrowheads point at the anterior paired dorsal aortae, outside of the hematopoietic PAS region. (ii,vi) *LacZ* expression in YS BI. (iii,vii) Expression in posterior paired dorsal aorta in the PAS region. Arrowheads indicate expression in the wall of the dorsal aortae. (iv and viii) Enlargement of boxed areas in panels iii and vii, respectively. Photographs in panels i and v were made using a 1.6× objective lens; panels ii-iv and vi-viii: 20× Nomarski objective. (C) *LacZ* expression in E10 *hsp68LacZ* + *23* F0 transgenic (i-iv) and *Runx1-lacZ* KI (v-viii) embryos. (i,v) Expression in the aorta in the AGM region (dorsal = up). Arrowhead in panel Ci indicates + 23 enhancer activity in a cluster of hematopoietic cells. *LacZ* expression is also seen in few individual cells in the endothelial layer and the mesenchyme (arrows). *LacZ* expression in the *Runx1-LacZ* KI (v) also includes a wider population of endothelial and mesenchymal cells. (ii,vi) Expression in hematopoietic cell clusters of the umbilical artery (arrowheads) and cells in the endothelial wall (arrows). (iii,vii) Expression in YS blood cells. (iv,viii) *LacZ* expression in FL. Black arrowheads indicate expression in individual hematopoietic cells. The white arrowhead points at the FL capsule. Original magnification, ×200.

When assayed in transient transfections in 416B cells, the full-length fragment resulted in a 7.2 (± 3.2)-fold (mean ± SD) increase in luciferase activity over the pGL3P control (Figure 3B). All of this activity was restricted to the central part (nt's 144-378) that spanned the mouse-frog conserved Gumby CNE. The less conserved 234 and 180 bp at the 5′ and 3′ end, respectively, were devoid of enhancer activity. Indeed, these parts may inhibit enhancer activity in vitro, as the central part alone resulted in approximately 2.4-fold higher luciferase activity than the full-length + 23 enhancer ($P = .02$; 2-tailed t test).

In the central part of the + 23 enhancer, we observed at least 7 frog-conserved phylogenetic footprints, 4 of which contained exact matches to consensus TF sites[32] for Myb (YAACNG), Runx (ACCRCA), Gata (WGATAR), or Ets (GGAW; Figure 4). In addition, there were less deeply conserved consensus Ets and E-box (CANNTG) motifs. Each of these motifs (apart from the E-box[33]) were mutated individually to assess their contribution to + 23 enhancer function. Most strikingly, mutation of the putative Runx or Gata site abolished all in vitro enhancer activity, resulting in luciferase levels comparable with the pGL3P control (Figure 3C). In addition, mutation of the most 5′ Ets site significantly lowered enhancer activity and this decreased even further when all 3 Ets motifs were mutated. Individual mutation of the other 2 Ets sites did not affect enhancer activity, neither did mutation of the Myb site or motif B or C. A minor decrease in activity was seen upon mutation of motif A. In conclusion, our data showed that the + 23 *Runx1* enhancer critically depends on deeply conserved Gata, Runx, and Ets motifs for its in vitro function. Whether other sequences in motifs A, B, and C or additional, less conserved sequences in the enhancer also are required for its function remains to be established. In addition, some of the conserved motifs may

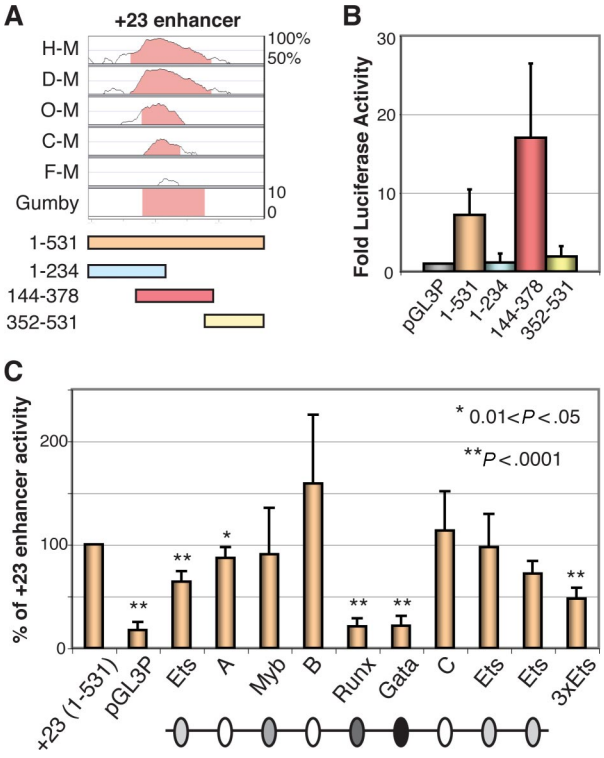

Figure 3. In vitro analysis of a + 23 *Runx1* enhancer deletion and mutation series. (A) Six-species VISTA output for the + 23 mouse-frog conserved CNE. Conservation over more than 100 bp and more than 70% is indicated in pink. A deletion series was generated as shown (colored boxes; nucleotide positions of fragments in full-length enhancer are indicated). (B) Dual luciferase assays in 416B cells showed that all in vitro + 23 enhancer activity resides in the 235-bp central, most conserved segment (nt's 144-378). Luciferase activity (corrected for transfection efficiency) was normalized to the enhancerless pGL3P vector. Data are the mean (± SD) of at least 4 independent transfections, using at least 2 separately prepared batches of test plasmid. (C) The + 23 enhancer is dependent on intact Runx, Gata, and Ets motifs for its activity in 416B cells. Luciferase activity of mutated constructs (corrected for transfection efficiency) was normalized to the activity of the nonmutated + 23 enhancer. Data are the mean (± SD) of at least 6 independent transfections (apart from the constructs carrying a mutation in the Myb [n = 4] and single 3′Ets site [n = 3]), using at least 2 separately prepared batches of test plasmid. * and ** indicate significant changes from the nonmutated + 23 enhancer (2-tailed Student *t* test).

have a positive or negative effect on enhancer activity in other cell types.

Binding of Gata, SCL, Ets, and Runx TFs to the + 23 enhancer in vivo

To explore whether Gata, Runx, and Ets TFs are recruited to the + 23 enhancer in vivo, we performed ChIP assays in 416B cells. ChIP samples were analyzed by real-time PCR for enrichment of + 23 enhancer sequences over control sequences located approximately 1-kb upstream and downstream of the enhancer, and at 2 CNEs 14.5- and 47.9-kb downstream of the enhancer, which we assumed to be devoid of hematopoietic *cis*-regulatory function as they lacked DHS (Figure 5A). ChIP experiments for Gata2, Runx1, Fli-1, Elf-1, and Pu.1 revealed that the + 23 *Runx1* enhancer was specifically enriched compared with the surrounding DNA and the no-antibody control (Figure 5B), confirming the in vivo binding of Gata2, Runx1, and Ets TFs to the enhancer. In hematopoiesis, SCL is frequently found in a complex with Gata factors,[24] so the presence of Gata2 at the + 23 *Runx1* enhancer (and the E-box motif) prompted us to examine whether an SCL complex is also recruited. Indeed, ChIP for SCL, Lmo2, and Ldb1 showed strong enrichments for all 3 TFs at the + 23 enhancer (Figure 5B).

The Runx motif is not critical to + 23 enhancer activity in the embryo

The need for an intact Runx motif for enhancer function and the binding of Runx1 in vivo suggested that a positive autoregulatory loop acts on the + 23 element in 416B cells. To examine whether the + 23 enhancer is subject to such a loop at the onset of hematopoiesis in the embryo, F0 transgenic embryos carrying the *hsp68LacZ + 23* enhancer-reporter construct with a mutated Runx motif (*hsp68LacZ + 23*^{Runx}) were generated and analyzed for *LacZ* expression as before. We found that the Runx mutation did not affect overall enhancer activity at the time of *Runx1* expression initiation in the embryo (early E8), or at stages of HSC emergence in the dorsal aorta and VU (E10) (compare Figures 6A and 2A). Indeed, the Runx-mutated enhancer was still active in the E8 PAS and in YS BIs (Figures 6Bi,ii and S3Ai). At E10, *LacZ* expression was still observed in the hematopoietic clusters of the dorsal aorta and VU (though expression levels in the dorsal aorta appeared somewhat decreased at this stage; Figure S3Bi,ii).

Activity of the + 23 *Runx1* enhancer in the embryo is controlled by Gata and Ets motifs

Since Gata and Ets motifs were critical for enhancer function in vitro, we examined whether these motifs are also important for the activity of the + 23 *Runx1* enhancer at the onset of hematopoiesis in the embryo. Mutation of the Gata site *(hsp68LacZ + 23*^{Gata}*)* resulted in complete abrogation of typical + 23 enhancer activity in the embryo (compare Figures 6A and 2A). In 2 of 6 E8 *hsp68LacZ + 23*^{Gata} F0 embryos, we observed nontypical *lacZ*

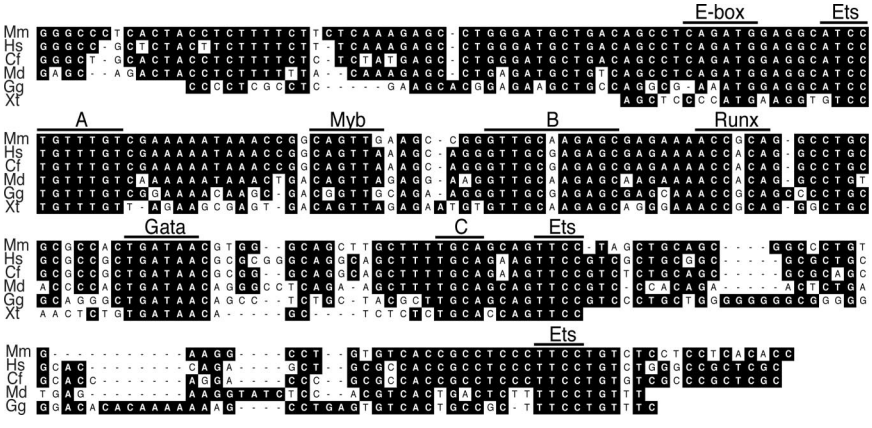

Figure 4. Six-species alignment of the central 235 bp of the + 23 *Runx1* enhancer. A stretch of 127 bp is conserved down to frog with 64% sequence identity. Within this stretch, phylogenetic footprints without (A-C) and with exact matches to predicted consensus TF-binding sites are indicated. In addition, mouse-chicken conserved Ets motifs at the 5′ and 3′ end of the enhancer fragment, and a mouse-opossum conserved E-box, are indicated. Mm indicates *Mus musculus;* Hs, *Homo sapiens;* Cf, *Canis familiaris;* Md, *Monodelphis domestica;* Gg, *Gallus gallus;* and Xt, *Xenopus tropicalis.*

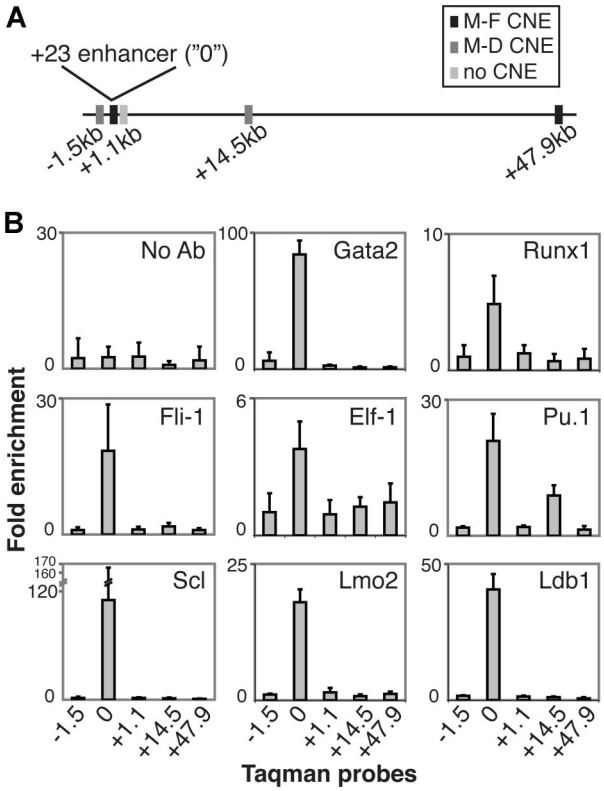

Figure 5. In vivo TF binding at the + 23 *Runx1* enhancer. (A) Schematic representation of the relative positions of 5 Taqman probes in *Runx1* intron 1 and surrounding the + 23 enhancer. Overlap of probes with CNEs as indicated. M indicates mouse; D, dog; and F, frog. (B) Real-time PCR analysis of ChIP with antibodies directed against Gata2, Runx1, Fli-1, Elf-1, Pu.1, Scl, Lmo2, and Ldb1 in 416B cells. A no-antibody (no Ab) control was included in each ChIP experiment. Data are the mean (± SD) from 2 (Gata2, Runx1, Fli-1, Elf-1, Pu.1, Scl) or one (Lmo2, Ldb1) independent ChIP with 3 real-time PCR assays per ChIP.

expression in the dorsolateral mesenchyme that extended into the wall of the dorsal aorta (Figure 6Biv). In addition, rare *LacZ*-expressing YS endodermal cells, but not cells in the BI (Figure 6Biii), were still present in one third of the embryos (Figure S3Aii). In all E10 F0 transgenic embryos, *LacZ* expression was completely lost from the clusters of hematopoietic cells in the dorsal aorta and VU, though faint expression was observed in some endothelial cells of the dorsal aorta and VU, in 2 of 6 and 1 of 6 embryos, respectively (Figure 6A; Figure S3Biii). None of the E10 embryos expressed *LacZ* in peripheral blood (PB) cells, the yolk sac, or fetal liver in a pattern relevant to the + 23 *Runx1* enhancer (ie, in individual hematopoietic cells).

Mutation of the 3 mouse-chicken/frog conserved Ets motifs in the + 23 *Runx1* enhancer *(hsp68LacZ + 23^{Ets})* also resulted in a severe reduction of *LacZ* expression in F0 transgenic embryos. In only 1 (13%) of 8 E8 embryos, *LacZ* was expressed in the posterior dorsal aorta versus 80% of embryos carrying the unmutated + 23 enhancer (compare Figures 6A and 2A). Moreover, this expression was weak and punctuate compared with the more uniform cytoplasmic expression seen with the unmutated + 23 enhancer (compare Figure 6Bvi with Figure 2Biii-iv). Weak, punctuate *LacZ* expression was also observed in the YS BIs of 25% of the E8 embryos, compared with strong YS BI expression in 80% of the *hsp68LacZ + 23* controls (compare Figures 6Bv, 2Bi,ii and S3Aiii). At E10, *LacZ* expression in hematopoietic clusters of the dorsal aorta was observed in only 1 of 7 embryos (Figures 6A and S3Biv). Similarly, expression in blood cells in the lumen of YS

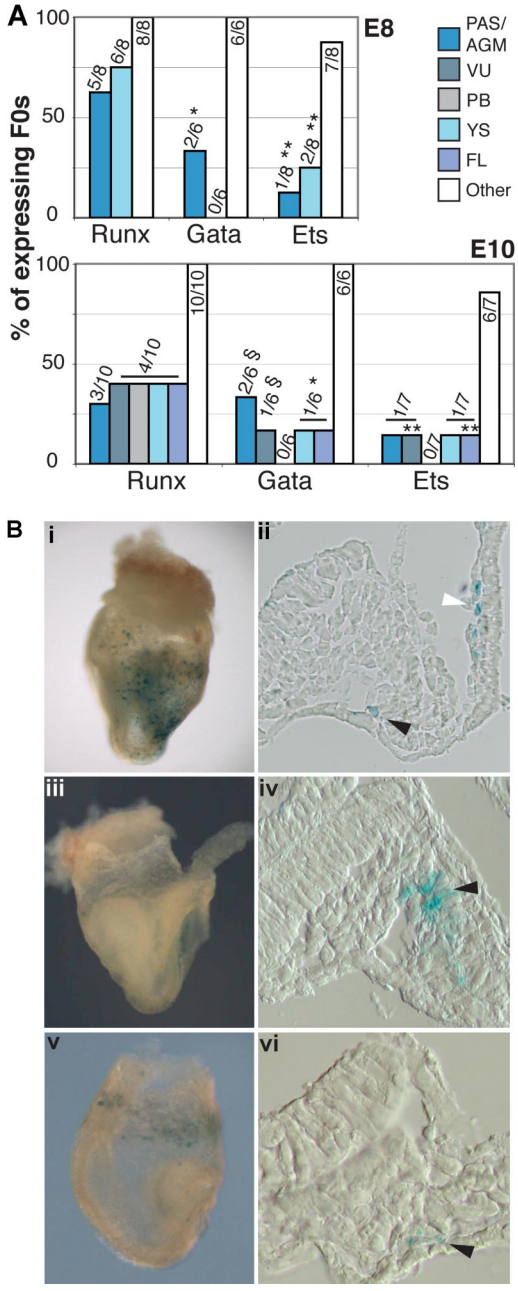

Figure 6. + 23 *Runx1* enhancer activity in hematopoietic tissues of the embryo critically depends on intact Gata and Ets motifs. (A) Summary of Runx, Gata, and Ets mutated + 23 enhancer activity in mouse embryos. Data show the number and percentage of embryos in which *LacZ* expression was found in the indicated tissue. YS indicates expression in E8 BI or E10 hematopoietic cells. "Other" represents ectopic, nonreproducible expression outside the hematopoietic system, resulting from random integration of the constructs at or near endogenous enhancers. *Observed expression is not typical to + 23 enhancer/endogenous *Runx1*. **Observed expression was punctuate and faint compared with the nonmutated + 23 enhancer. §Observed expression was faint and restricted to a subset of endothelial cells. (B) Effects of Runx, Gata and Ets mutations on + 23 enhancer activity in E8 embryos. (i,ii) *hsp68LacZ + 23^{Runx}* F0 transgenic embryo. (i) Whole mount, showing expression in the YS. (ii) Section through the PAS and YS. Black arrowhead indicates *LacZ* expression in paired dorsal aortae; white arrowhead points at expressing cells in BI. (iii,iv) *hsp68LacZ + 23^{Gata}* F0 embryo. Arrowhead points at cells in the dorsolateral mesenchyme of the PAS that expresses *LacZ*. (v-vi) *hsp68LacZ + 23^{Ets}* F0 embryo. Arrowhead points at faint, punctuate *LacZ* expression in the wall of the dorsal aorta. (ii,iv,vi) Original magnification, ×200.

capillaries was seen in 1 of 7 embryos. In none of the E10 embryos did we observe any *LacZ*-expressing PB cells or + 23-specific enhancer activity in the VU or FL.

The + 23 enhancer is active in clonogenic progenitors and definitive HSCs in the embryo

To demonstrate unambiguously that the + 23 *Runx1* enhancer is active in hematopoietic progenitor and stem cells of the midgestation embryo, E11 dorsal aorta + VU (AVU) and FL cells were assayed for the presence of in vitro clonogenic progenitor cells (colony-forming unit–culture, CFU-C) and in vivo long-term multilineage reconstituting HSC (LTR-HSC) activity. For this, an *hsp68LacZ + 23* transgenic mouse line, *+ 23-Line1* (Figure S4), was used. Flow cytometric analysis of FDG-loaded E11 AVU and FL cells showed that the + 23 enhancer was active in on average 2.8% (± 1.2%) of AVU cells (mean ± SD; n = 13) and 37.8% (± 4.3%) of FL cells (n = 10) (Figure 7A; FDG is a fluorescent substrate for β-galactosidase). FDG^+ and FDG^- cells were sorted from the AVU and FL cell suspensions and assayed for the presence of CFU-Cs. We found that the FDG^+ population was on average 47.1-fold (AVU) and 3.1-fold (FL) enriched for CFU-Cs (Figure 7B). Calculation of the absolute number of FDG^+ and FDG^- CFU-Cs per embryo showed that the majority of AVU and FL CFU-Cs were present in the FDG^+ population (Figure 7C).

To assay for LTR-HSC activity, sorted FDG^+ and FDG^- cells were transplanted into irradiated adult recipients. Analysis of recipient PB at more than 4 months after transfer showed that donor-derived PB reconstitution was predominantly found among the mice that received a transplant of FDG^+ AVU or FL cells (Figure 7D). Moreover, FDG^+ cells conferred high-level PB reconstitution (> 50%; Figure 7E), and contributed to all hematopoietic tissues and lineages analyzed (Figure 7F,G). This is indicative of the presence of bona fide LTR-HSCs in the FDG^+ subset. Of the 18 recipients that received a transplant of FDG^- AVU or FL cells, only 1 contained donor-derived PB cells (contributing to 20% of PB; Figure 7D,E). It cannot be excluded that a few contaminating FDG^+ cells in the FDG^- population are responsible for this (sort purity of the FDG^- cells in this experiment was 97.5%). Thus, we conclude that the + 23 *Runx1* enhancer is active in the majority of CFU-Cs and in most, if not all, definitive HSCs of the E11 AVU and FL.

Discussion

Until our study, little was known about the direct transcriptional regulation of *Runx1* expression and thus its place in the genetic pathways that govern definitive HSC emergence. This is surprising, as *Runx1* is a (if not "the") master regulator of definitive blood formation in the embryo. The results presented here now provide a better understanding of the transcriptional regulation of *Runx1* during the onset of hematopoiesis, and in particular HSC generation in the mouse embryo. Using a combination of comparative genomics and functional assays, we have successfully isolated a *Runx1* intronic *cis*-regulatory element (named the + 23 *Runx1* enhancer) that is active from the initiation of *Runx1* expression in the E8 PAS until its expression in definitive HSCs and progenitors in hematopoietic clusters of the dorsal aorta and VU and in the FL. Importantly, we have identified Gata2 and Ets transcription factors as direct upstream regulators of *Runx1*.

Runx1 candidate regulatory elements

The Gumby algorithm[21] was used to identify CNEs with a high likelihood of function. In our alignment of the *Runx1* loci of 6 vertebrate species, Gumby detected 13 mouse-frog CNEs with *P* values less than le-10. The *Runx1* P1, P2, and the + 23 enhancer described here comprise 3 of these. As the *Runx1* + 23 enhancer did not target reporter gene expression to the nonhematopoietic *Runx1*-expressing tissues[6] of the embryo, the remaining CNEs are likely to reflect additional tissue-specific *Runx1 cis*-elements, similar to what was described for other developmental regulated gene loci.[21]

Specificity for HSCs and hematopoietic progenitor cells

We showed that the 531-bp + 23 *Runx1* enhancer targets reporter gene expression to all known hematopoietic tissues of the mouse embryo in a spatiotemporal pattern that is specific and consistent with the hematopoietic expression of the endogenous *Runx1* gene[23,28,30,31,34,35] (and this study). Moreover, we demonstrated unambiguously that the + 23 enhancer is active in definitive HSCs and clonogenic progenitors of the dorsal aorta, VU, and FL. In line with this, the + 23 *Runx1* enhancer particularly targeted reporter gene expression to the clusters of hematopoietic cells protruding from the walls of the aorta and VU where HSCs were previously found.[27,28] Interestingly, reporter gene–marked clusters were present not only at the ventral wall of the dorsal aorta (where hematopoietic clusters were historically described[4]), but also along its dorsal wall. Recently, Taoudi and Medvinsky [36] reported on the presence of clusters at the dorsal wall of the mouse aorta, and showed that this side of the vessel contains clonogenic hematopoietic progenitor cells, while the ventral aortic wall harbors definitive HSCs as well as clonogenic progenitors. Together, these data indicate that the + 23 *Runx1* enhancer faithfully targets the emerging hematopoietic stem and progenitor cells on both sides of the dorsal aorta.

The + 23 *Runx1* enhancer as a tool to study developmental origins of HSCs

The + 23 *Runx1* enhancer also targeted *lacZ* expression to a few cells of the endothelium and mesenchyme of the E10 dorsal aorta, but did not recapitulate the wider endothelial/mesenchymal endogenous *Runx1* expression (compare Figure 2Ci,v). We observed this enhancer-specific *LacZ* expression pattern not only in F0 embryos but also in 4 independently generated transgenic mouse lines, and therefore concluded that it truly reflects the intrinsic activity of the enhancer. This more restricted activity of the + 23 enhancer compared with endogenous *Runx1* suggests that it may target only those aortic endothelial/mesenchymal *Runx1*-expressing cells that are the precursors of the HSCs and clonogenic progenitors (ie, the proposed hematogenic endothelium/hemangioblasts).[4,23,28] Interestingly, it was shown recently that endogenous *Runx1*-expressing cells of the E7.5 to E8.5 mouse conceptus contributed to the definitive bone marrow HSC pool.[35] The early onset of + 23 enhancer activity and endogenous *Runx1* expression in a few cells in the wall of the dorsal aortae of the E8 to E8.5 PAS suggests that these are (part of) the cells responsible for this contribution. A thorough analysis of the nature and fate of the cells in which the + 23 *Runx1* enhancer is specifically active in the E8 embryo will be instrumental in addressing this notion.

The + 23 *Runx1* enhancer integrates Gata, Ets, and SCL transcriptional pathways during HSC formation

Mutation analyses of the + 23 *Runx1* enhancer revealed that deeply conserved Gata and Ets motifs are essential for its

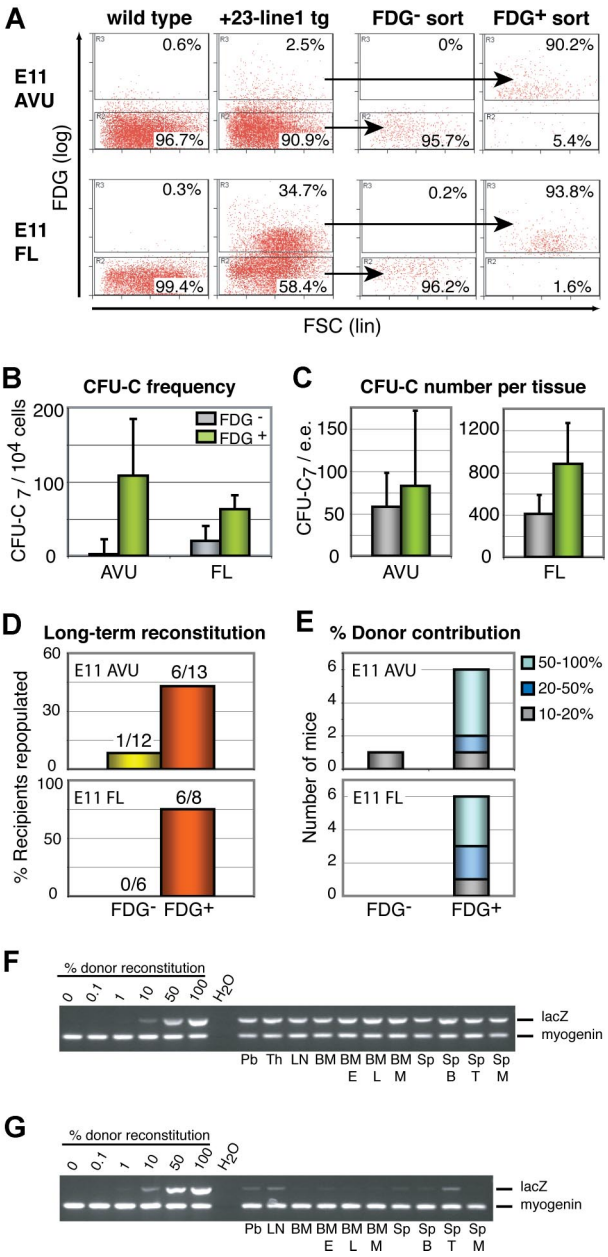

Figure 7. The + 23 *Runx1* enhancer targets *LacZ* expression to clonogenic progenitors and definitive LTR-HSCs in the E11 AVU and FL of + *23-Line1* transgenic embryos. (A) Representative dot plots of + 23 enhancer activity (measured by FDG). FDG-loaded tissues of wild-type littermates are shown as negative control. Sort gates as indicated. Purity of sorted populations was 96% (± 2.7%; mean ± SD; n = 13) and 86.0% (± 5.8%; n = 9) for AVU FDG$^-$ and FDG$^+$ cells, respectively, and 95.4% (± 3.1%; n = 10) and 85.8% (± 11.3%; n = 10) for FL FDG$^-$ and FDG$^+$ cells, respectively. (B,C) Analysis of clonogenic progenitors (CFU-C_7) among AVU and FL FDG$^-$ and FDG$^+$ cells. (B) Frequency of CFU-C_7 in each population tested (mean ± SD). (C) Absolute number of CFU-C_7 per embryo equivalent of AVU and FL FDG$^-$ and FDG$^+$ cells (mean ± SD; n = 3). (D) LTR-HSC activity in AVU and FL FDG$^-$ and FDG$^+$ cell populations. Frequency and absolute numbers of mice showing more than 10% PB donor-derived reconstitution at more than 4 months after transfer. (E) Percentage donor contribution in reconstituted mice as determined by semiquantitative PCR for the donor genetic marker in PB genomic DNA. (F,G) Multilineage analysis of recipients of FDG$^+$ AVU cells with more than 50% donor-derived PB cells (F) and more than 10% donor-derived PB cells (G). In both cases, donor cells contributed to all hematopoietic tissues and lineages analyzed. Pb indicates peripheral blood; Th, thymus; LN, mesenteric lymph node; BM, bone marrow; Sp, spleen; E, erythroid cells; L, bone lymphoid cells; M, myeloid cells; B, B cells; and T, T cells. Percent donor reconstitution was determined by comparison with standards containing 0%, 0.1%, 1%, 10%, 50%, and 100% of donor genomic DNA.

activity at the onset of hematopoiesis. Moreover, ChIP experiments showed that Gata2, the Ets factors Fli-1, Elf-1, Pu.1, and the SCL/Lmo2/Ldb1 complex, are bound to the enhancer in vivo. Although we did not mutate the E-box in the + 23 enhancer, support that SCL is a direct regulator of *Runx1* in developmental hematopoiesis comes from studies in zebrafish.[12,13] In addition, a search for SCL target genes in mouse identified *Runx1* as a direct target in YS and FL (J.-R. Landry, S. Kinston, K. Knezevic, M.F.T.R.B., N. Wilson, W.T.N., F. Edenhofer, J. E. Pimanda, and B. Gottgens, manuscript submitted, July 2007). Together, this indicates that the activity of the + 23 *Runx1* enhancer is regulated by Gata, Ets, and SCL TFs. Gata2, Fli-1, and the SCL complex are themselves important regulators of developmental hematopoiesis[1,37-41] (and references therein). We showed here that the + 23 *Runx1* enhancer has a more restricted activity in the dorsal aorta than the previously identified Gata2, Fli-1, or SCL enhancers,[25,42-46] in that it targets mainly emerging hematopoietic clusters and not the general endothelium. The deeply conserved TF motifs and their precise spacing in the + 23 enhancer are likely to dictate the specific stoichiometry and temporal binding of a Gata2, Fli-1, and SCL containing protein complex (see also Anguita et al[24]; Hughes et al[47]; and Ferreira et al[48]). We suggest that it is the precise spatiotemporal expression of all 3 TFs that controls *Runx1* expression and thus the fate of precursor cells to commit to the hematopoietic lineage. In addition, other as-yet-unidentified motifs may contribute to the specificity of the enhancer, either in a positive way or by recruiting repressors in cells in which the + 23 *Runx1* enhancer is inactive but Gata, Ets, and Scl TF are present.

Autoregulation via the + 23 enhancer

Our data suggest that the + 23 enhancer is subject to a Runx1 autoregulatory loop in adult-derived 416B cells. However, analysis of *hsp68LacZ* + *23^{Runx}* F0 transgenic embryos provided no support for *Runx1* autoregulation through the + 23 enhancer at the onset of hematopoiesis. Analysis of + 23 enhancer activity on a *Runx1*-null background confirmed and extended this finding as *LacZ* expression in the YS BI and wall of the E8 paired dorsal aortae was not affected in these embryos (A.C. Santos and M.F.T.R.B, unpublished observations, October 2006). However, it cannot be excluded that the + 23 enhancer is subject to Runx1 autoregulation at later developmental time points. In such an autoregulatory loop, Runx1 may act with Gata factors to maintain *Runx1* expression during terminal differentiation of specific cell types.[49,50]

Conclusion

We have identified and characterized a hematopoietic-specific *Runx1* enhancer that is active during the onset of mouse hematopoiesis and critically requires Gata and Ets motifs for its activity. Importantly, we showed that the + 23 *Runx1* enhancer marks bona fide HSCs at their site of generation in the dorsal aorta and VU, and in the FL, unambiguously implicating this enhancer in the process of HSC generation. Finally, our data indicate that Gata2, Fli-1, and the SCL complex are recruited to the + 23 enhancer in vivo, placing *Runx1* directly downstream of these factors in the transcriptional network that governs HSC emergence.

Acknowledgments

This work was supported by the Medical Research Council (W.T.N., A.J., C.L.S., P.-S.L., J.S.-S., M.F.T.R.B.) and the Programs for Genomic Applications (grant HL066681) (J-F.C., S.P., and E.M.R.) of the National Institutes of Health National Heart, Lung and Blood Institute.

We are grateful to Bill Wood, Dies Meijer, Elaine Dzierzak, Roger Patient, Jim Hughes, and Doug Higgs for advice and for critical comments on the paper. We also thank past and present members of the de Bruijn laboratory for their help and discussions; the Higgs laboratory for advice on chromatin analyses; Ann Atzberger for flow cytometry; Bertie Gottgens for stimulating discussions; the Computational Biology Research Group, Nicki Ventress, and Ilya Malinov for bioinformatics assistance; Jackie Sharpe and Bill Wood for efficiently managing the mouse transgenesis unit; Frank Grosveld and Elaine Dzierzak for their support in generating transgenics; and Colin Hetherington and staff for Biomedical Services.

Authorship

Contribution: W.T.N. performed the research, analyzed the data, and drafted the paper; A.J., M.B., and C.L.S. performed research and analyzed data; J.-F.C., S.P., and E.M.R. contributed vital genomic sequences and bioinformatic analysis tools; P.-S.L., J.S.-S., and J.K.-S. generated transgenics; M.F.T.R.B. designed the study, performed research, analyzed data, and wrote the paper.

Conflict-of-interest disclosure: The authors declare no competing financial interests.

Correspondence: M. de Bruijn, MRC Molecular Haematology Unit, Weatherall Institute of Molecular Medicine, John Radcliffe Hospital, Oxford OX3 9DS, United Kingdom; e-mail: marella.debruijn@imm.ox.ac.uk.

References

1. Swiers G, Patient R, Loose M. Genetic regulatory networks programming hematopoietic stem cells and erythroid lineage specification. Dev Biol. 2006;294:525-540.
2. Soneji S, Huang S, Loose M, et al. Inference, validation and dynamic modelling of transcription networks in multipotent hematopoietic cells. Ann N Y Acad Sci. 2007;1106:30-40.
3. de Bruijn MF, Speck NA. Core-binding factors in hematopoiesis and immune function. Oncogene. 2004;23:4238-4248.
4. Jaffredo T, Nottingham W, Liddiard K, Bollerot K, Pouget C, de Bruijn M. From the hemangioblast to the hematopoietic stem cell: an endothelial connection? Exp Hematol. 2005;33:1029-1040.
5. Speck NA, Gilliland DG. Core-binding factors in haematopoiesis and leukaemia. Nat Rev Cancer. 2002;2:502-513.
6. Levanon D, Groner Y. Structure and regulated expression of mammalian RUNX genes. Oncogene. 2004;23:4211-4219.
7. Kumano K, Chiba S, Kunisato A, et al. Notch1 but not Notch2 is essential for generating hematopoietic stem cells from endothelial cells. Immunity. 2003;18:699-711.
8. Hadland BK, Huppert SS, Kanungo J, et al. A requirement for Notch1 distinguishes 2 phases of definitive hematopoiesis during development. Blood. 2004;104:3097-3105.
9. Gering M, Patient R. Hedgehog signaling is required for adult blood stem cell formation in zebrafish embryos. Dev Cell. 2005;8:389-400.
10. Burns CE, Traver D, Mayhall E, Shepard JL, Zon LI. Hematopoietic stem cell fate is established by the Notch-Runx pathway. Genes Dev. 2005;19:2331-2342.
11. Robert-Moreno A, Espinosa L, de la Pompa JL, Bigas A. RBPjkappa-dependent Notch function regulates Gata2 and is essential for the formation of intra-embryonic hematopoietic cells. Development. 2005;132:1117-1126.
12. Patterson LJ, Gering M, Patient R. Scl is required for dorsal aorta as well as blood formation in zebrafish embryos. Blood. 2005;105:3502-3511.
13. Patterson LJ, Gering M, Eckfeldt CE, et al. The transcription factors Scl and Lmo2 act together during development of the hemangioblast in zebrafish. Blood. 2007;109:2389-2398.
14. Nakagawa M, Ichikawa M, Kumano K, et al. AML1/Runx1 rescues Notch1-null mutation-induced deficiency of para-aortic splanchnopleural hematopoiesis. Blood. 2006;108:3329-3334.
15. Pimanda JE, Donaldson IJ, de Bruijn MF, et al. The SCL transcriptional network and BMP signaling pathway interact to regulate RUNX1 activity. Proc Natl Acad Sci U S A. 2007;104:840-845.
16. National Center for Biotechnology Information. Mapviewes. http://www.ncbi.nlm.nih.gov/mapview/. Accessed August 2006.
17. Sanger Institute. Ensembl. http://www.ensembl.org/index.html. Accessed August and November 2006.
18. Brudno M, Do CB, Cooper GM, et al. LAGAN and Multi-LAGAN: efficient tools for large-scale multiple alignment of genomic DNA. Genome Res. 2003;13:721-731.
19. Frazer KA, Pachter L, Poliakov A, Rubin EM, Dubchak I. VISTA: computational tools for comparative genomics. Nucleic Acids Res. 2004;32:W273-W279.
20. Schwartz S, Zhang Z, Frazer KA, et al. PipMaker: a web server for aligning two genomic DNA sequences. Genome Res. 2000;10:577-586.
21. Prabhakar S, Poulin F, Shoukry M, et al. Close sequence comparisons are sufficient to identify human cis-regulatory elements. Genome Res. 2006;16:855-863.
22. Sandelin A, Alkema W, Engstrom P, Wasserman WW, Lenhard B. JASPAR: an open-access database for eukaryotic transcription factor binding profiles. Nucleic Acids Res. 2004;32:D91-D94.
23. North T, Gu TL, Stacy T, et al. Cbfa2 is required for the formation of intra-aortic hematopoietic clusters. Development. 1999;126:2563-2575.
24. Anguita E, Hughes J, Heyworth C, Blobel GA, Wood WG, Higgs DR. Globin gene activation during haemopoiesis is driven by protein complexes nucleated by GATA-1 and GATA-2. EMBO J. 2004;23:2841-2852.
25. Gottgens B, Nastos A, Kinston S, et al. Establishing the transcriptional programme for blood: the SCL stem cell enhancer is regulated by a multiprotein complex containing Ets and GATA factors. EMBO J. 2002;21:3039-3050.
26. de Bruijn MF, Speck NA, Peeters MC, Dzierzak E. Definitive hematopoietic stem cells first develop within the major arterial regions of the mouse embryo. EMBO J. 2000;19:2465-2474.
27. de Bruijn MF, Ma X, Robin C, Ottersbach K, Sanchez MJ, Dzierzak E. Hematopoietic stem cells localize to the endothelial cell layer in the midgestation mouse aorta. Immunity. 2002;16:673-683.
28. North TE, de Bruijn MF, Stacy T, et al. Runx1 expression marks long-term repopulating hematopoietic stem cells in the midgestation mouse embryo. Immunity. 2002;16:661-672.
29. Ghozi MC, Bernstein Y, Negreanu V, Levanon D, Groner Y. Expression of the human acute myeloid leukemia gene AML1 is regulated by two promoter regions. Proc Natl Acad Sci U S A. 1996;93:1935-1940.
30. Ottersbach K, Dzierzak E. The murine placenta contains hematopoietic stem cells within the vascular labyrinth region. Dev Cell. 2005;8:377-387.
31. Zeigler BM, Sugiyama D, Chen M, Guo Y, Downs KM, Speck NA. The allantois and chorion, when isolated before circulation or chorio-allantoic fusion, have hematopoietic potential. Development. 2006;133:4183-4192.
32. Wang H, Zhang Y, Cheng Y, et al. Experimental validation of predicted mammalian erythroid cis-regulatory modules. Genome Res. 2006;16:1480-1492.
33. Porcher C, Liao EC, Fujiwara Y, Zon LI, Orkin SH. Specification of hematopoietic and vascular development by the bHLH transcription factor SCL without direct DNA binding. Development. 1999;126:4603-4615.
34. Lacaud G, Gore L, Kennedy M, et al. Runx1 is essential for hematopoietic commitment at the hemangioblast stage of development in vitro. Blood. 2002;100:458-466.
35. Samokhvalov IM, Samokhvalova NI, Nishikawa S. Cell tracing shows the contribution of the yolk sac to adult haematopoiesis. Nature. 2007;446:1056-1061.
36. Taoudi S, Medvinsky A. Functional identification of the hematopoietic stem cell niche in the ventral domain of the embryonic dorsal aorta. Proc Natl Acad Sci U S A. 2007;104:9399-9403.
37. Ling KW, Ottersbach K, van Hamburg JP, et al. GATA-2 plays two functionally distinct roles during the ontogeny of hematopoietic stem cells. J Exp Med. 2004;200:871-882.
38. Oikawa T, Yamada T. Molecular biology of the Ets family of transcription factors. Gene. 2003;303:11-34.
39. Lecuyer E, Hoang T. SCL: from the origin of hematopoiesis to stem cells and leukemia. Exp Hematol. 2004;32:11-24.

40. Meier N, Krpic S, Rodriguez P, et al. Novel binding partners of Ldb1 are required for haematopoietic development. Development. 2006;133:4913-4923.
41. Cumano A, Godin I. Ontogeny of the hematopoietic system. Annu Rev Immunol. 2007;25:745-785.
42. Minegishi N, Ohta J, Yamagiwa H, et al. The mouse GATA-2 gene is expressed in the para-aortic splanchnopleura and aorta-gonads and mesonephros region. Blood. 1999;93:4196-4207.
43. Minegishi N, Suzuki N, Yokomizo T, et al. Expression and domain-specific function of GATA-2 during differentiation of the hematopoietic precursor cells in midgestation mouse embryos. Blood. 2003;102:896-905.
44. Khandekar M, Brandt W, Zhou Y, et al. A Gata2 intronic enhancer confers its pan-endothelia-specific regulation. Development. 2007;134:1703-1712.
45. Gottgens B, Broccardo C, Sanchez MJ, et al. The scl +18/19 stem cell enhancer is not required for hematopoiesis: identification of a 5′ bifunctional hematopoietic-endothelial enhancer bound by Fli-1 and Elf-1. Mol Cell Biol. 2004;24:1870-1883.
46. Donaldson IJ, Chapman M, Kinston S, et al. Genome-wide identification of cis-regulatory sequences controlling blood and endothelial development. Hum Mol Genet. 2005;14:595-601.
47. Hughes JR, Cheng JF, Ventress N, et al. Annotation of cis-regulatory elements by identification, subclassification, and functional assessment of multispecies conserved sequences. Proc Natl Acad Sci U S A. 2005;102:9830-9835.
48. Ferreira R, Wai A, Shimizu R, et al. Dynamic regulation of Gata factor levels is more important than their identity. Blood. 2007;109:5481-5490.
49. Ferjoux G, Auge B, Boyer K, Haenlin M, Waltzer L. A GATA/RUNX cis-regulatory module couples Drosophila blood cell commitment and differentiation into crystal cells. Dev Biol. 2007;305:726-734.
50. Gajewski KM, Sorrentino RP, Lee JH, Zhang Q, Russell M, Schulz RA. Identification of a crystal cell-specific enhancer of the black cells prophenoloxidase gene in Drosophila. Genesis. 2007;45:200-207.

Erratum

In the article by Baumeister et al entitled "G-CSF mobilizes slanDCs (6-sulfo LacNAc$^+$ dendritic cells) with a high proinflammatory capacity," which appeared in the October 15, 2007, issue of *Blood* (Volume 110:3078-3081), Figure 1B contained duplicate histograms. The correct Figure 1B is shown here.

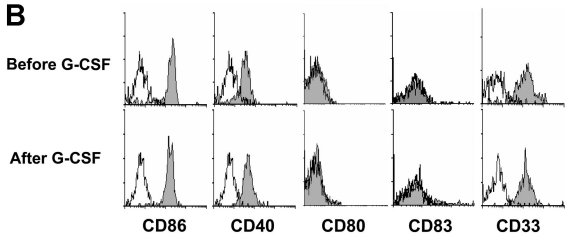

Figure 1B